Electronic Supplementary Information

Strategically Incorporated V in Rod-like Ni-MOF as an Effective Catalyst for Water Oxidation Reaction

Krishnendu Bera,[†‡] Suprobhat Singha Roy,[†‡] Ragunath Madhu,[†‡] Aditi De,[†‡] Pradeep Gudlur[$] and Subrata Kundu[†‡]*

[†]Academy of Scientific and Innovative Research (AcSIR), Ghaziabad-201002, India.

[‡]Electrochemical Process Engineering (EPE) Division, CSIR-Central Electrochemical Research Institute (CECRI), Karaikudi-630003, Tamil Nadu, India.

[$]Department of Mechanical Engineering, Union College, 807 Union Street Schenectady, NY, 12308, USA.

*To whom correspondence should be addressed, *E-mail:* skundu@cecri.res.in; kundu.subrata@gmail.com, Phone/Fax: (+ 91) 4565-241487.

This file contains pages from **S1 to S23**, where the detailed, reagents and instruments used in the study, figures, and Tables have been given.

Number of Pages: 23

Number of Figures: 14

Number of Tables: 02

Reagents and Instruments:

Nickel chloride ($NiCl_2$) and Vanadium chloride (VCl_3) were sourced from Sigma-Aldrich. Benzene tricarboxylic acid (BTC) was purchased from Sigma-Aldrich. All electrochemical characterizations were conducted using a Metrohm Autolab. The Hg/HgO as reference and Pt as counter (in 1 M KOH) were purchased from CH Instruments. A carbon cloth (CC) from Alfa-Aesar served as the working electrode. Throughout the experiments, DI water was used. The catalysts, prepared in various stoichiometric ratios, underwent characterization using HR-TEM (TecnaiTM G2 TF20 at 200 kV) and Talos F-200-S with HAADF elemental mapping. Colour mapping and EDS analysis were performed using the FESEM instrument (SUPRA 55VP Carl Zeiss) equipped with an EDS detector. The XRD scans were done at a rate of 5° min^{-1} within the 2θ range of 10-80° on a Rigaku X-ray diffractometer, using Cu Kα radiation. Lastly, XPS evaluations were executed on a Theta Probe AR-XPS system by Thermo Fisher Scientific, UK.

Electrochemical Characterizations:

Electrocatalytic investigations were performed using a conventional three-electrode setup. For the Oxygen Evolution Reaction (OER) experiments, Carbon cloth (CC) was employed as the counter electrode. The reference electrode chosen for OER was Hg/HgO. Polarization assessments were conducted at a deliberately slow scan rate of 5 mV/sec. A manual 85% iR compensation was applied, utilizing R_s data obtained from Electrochemical Impedance Spectroscopy (EIS). To assess accelerated degradation (AD), continuous rapid sweeps were conducted through 1000 cycles at a significantly high sweep rate of 150 mV s^{-1}, all within a 1 M KOH solution. Electrochemical impedance studies encompassed a frequency spectrum from 1 Hz to 100 kHz.

Electrode fabrication:

The electrodes were fabricated using the traditional drop-casting technique onto carbon cloth (CC) substrates. A catalytic ink was formulated by mixing water, ethanol, and nafion in a ratio of (7.5:2:0.5) to produce a 1 mL solution. Subsequently, 34.5 μL of the resulting solution was drop-casted onto the CC and then dried at a temperature of 60°C. The dried electrode thus prepared was employed as the working electrode (with a catalyst loading of 0.1 mg/cm^2) for the OER process.

C_{dl} Calculation:

The double layer capacitance (C_{dl}) was determined from a CV in the range of 0.2 to 0.3 V vs Hg/HgO electrode at a scan rate of 30, 60, 90, 120, and 150 mV/s, using the equation: C_{dl}= Δj (j_a-j_c)/2ν, where j_a and j_c are anodic and cathodic current densities and ν is the scan rate in mVs^{-1}. The non-Faradic current density-based electrochemically active surface area (ECSA) was estimated according to the equation: ECSA = C_{dl}/C_s, where Cs is the specific capacitance of the electrode in 1 M KOH electrolyte. Finally, we calculate Cdl using the slope of the graph Δj vs ν.

❖ **Determination of Surface concentration of various alloys from the redox features of CV:**

- Calculated area associated with the reduction of Ni^{3+} to Ni^{2+} of **Ni-BTC** = 0.000494 VA

Hence, the associated charge is = 0.000494VA / 0.005 Vs^{-1}

= 0.0988As

= 0.0988 C

Now, the number of electron transferred is = 0.0988 C / 1.602 ×10^{-19}

= **6.16729×10^{17}**

Given that the reduction of Ni^{3+} to Ni^{2+} involves a single electron transfer reaction, the quantity of electrons computed previously corresponds precisely to the count of active sites at the surface.

Hence, the number of Ni participating in OER is = **6.16729×10^{17}**

In our study, the determination of Turnover Frequency (TOF) from OER Current Density TOF was calculated assuming that the surface-active Co atoms that had undergone the redox reaction just before onset of OER only participated in OER electrocatalysis. The corresponding expression is,

$$TOF= (j \times N_A)/ (F \times n \times \Gamma)$$

Where, j = current density N_A= Avogadro number F = Faraday constant n = Number of electrons Γ = Surface concentration.

Hence, we have,

$TOF_{1.60\ V} = [(0.00985)\ (6.023\times 10^{23})] / [(96485)\ (4)\ (6.16729\times10^{17})]$

= **$0.024920845\ sec^{-1}$**

= **$89.71504041\ h^{-1}$**

- Calculated area associated with the oxidation of Ni^{3+} to Ni^{2+} of **NiV-BTC** = 0.00006 VA

Hence, the associated charge is = 0.00006 VA / 0.005 Vs^{-1}

= 0.012 As

= **0.012 C**

Now, the number of electron transferred is = $0.012/ 1.602 \times10^{-19}$

= **7.49064×10^{16}**

Given that the reduction of Ni^{3+} to Ni^{2+} involves a single electron transfer reaction, the quantity of electrons computed previously corresponds precisely to the count of active sites at the surface.

Hence, the number of Ni participating in OER is = **7.49064×10^{16}**

Hence, we have,

$TOF_{1.60\ V}$ = [(0.0238) (6.023× $10^{23)}$] / [(96485) (4) (7.49064×1016)]

= **0.495768788 sec^{-1}**

= **1784.767636 h^{-1}**

Activation energy calculation:

The temperature-dependent kinetic analysis was employed to assess the influence of V on the apparent activation energy (E_{app}) and pre-exponential factor (A_{app}) of NiV-BTC electrocatalysts. This analysis aimed to gain insights into how V affects the catalytic mechanism. Cyclic voltammetry (CV) curves were obtained for both Ni-BTC and NiV-BTC samples in a 1.0 M KOH solution over a temperature range of 25 to 50°C. As expected, the oxygen evolution reaction (OER) activities of both samples increased with rising temperature. The values of both catalysts at constant overpotentials were determined using the Arrhenius equation. This equation can be expressed as follows:

$$j = A_{app} \exp (E_{app}/RT)$$

Where:

j is the current density normalized by ECSA, k is the rate constant for the reaction, A is the pre-exponential factor (A_{app} in this case), E_{app} is the apparent activation energy, R is the universal gas constant (8.314 J/(mol·K)), T is the absolute temperature in Kelvin.

Thus, the Eapp values at different potentials can be calculated by fitting the slope of the Arrhenius curve by using the following equation:

$$\delta \ln(j)/ \delta(1/T) = - E_{app}/R$$

So, the slope of this equation is: Slope = E_{app}/R, and the intercept of ln(j) against 1/T curve is the ln (A_{app}).

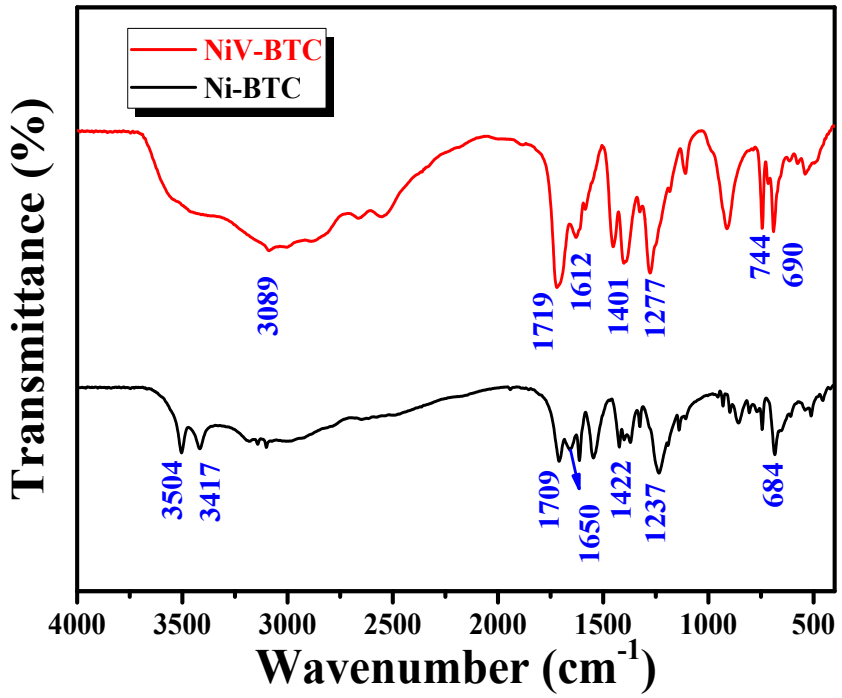

Figure S1: FT-IR spectrum of Ni-BTC and NiV-BTC.

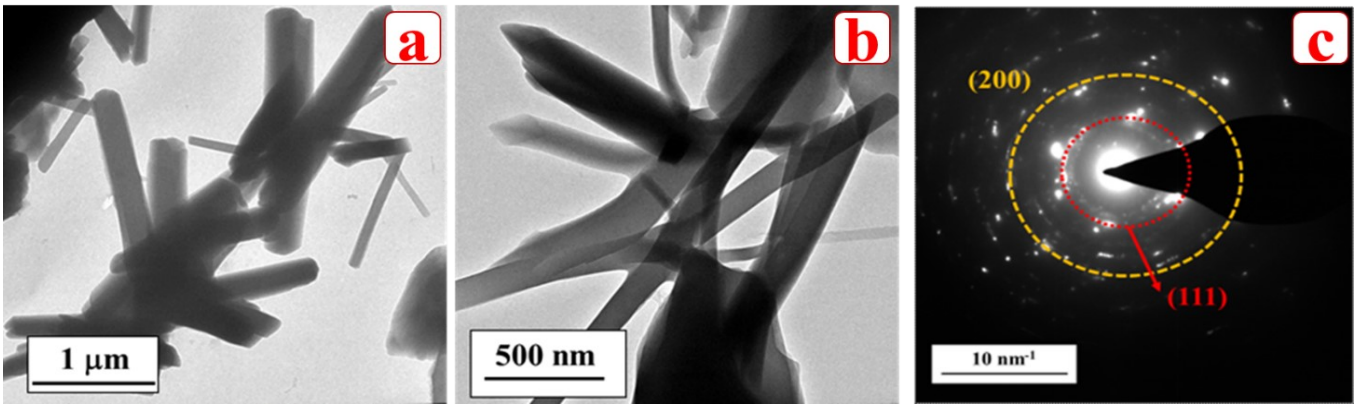

Figure S2: (a,b) Low to high magnification HR-TEM images of Ni-BTC, (c) SAED pattern of Ni-BTC.

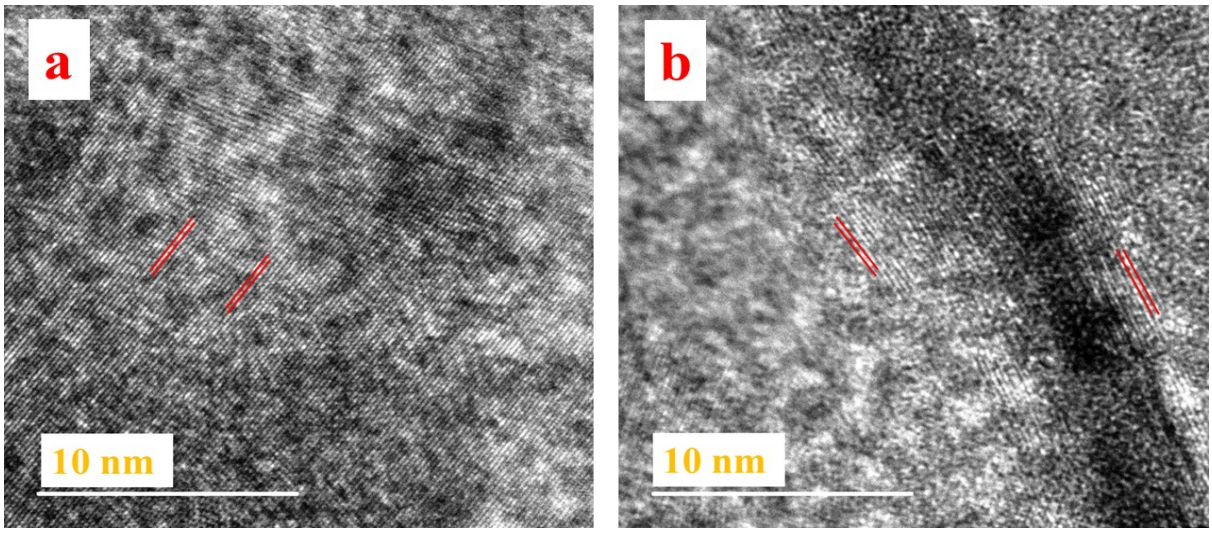

Figure S3: (a,b) Lattice fringes pattern of Ni-BTC and NiV-BTC respectively.

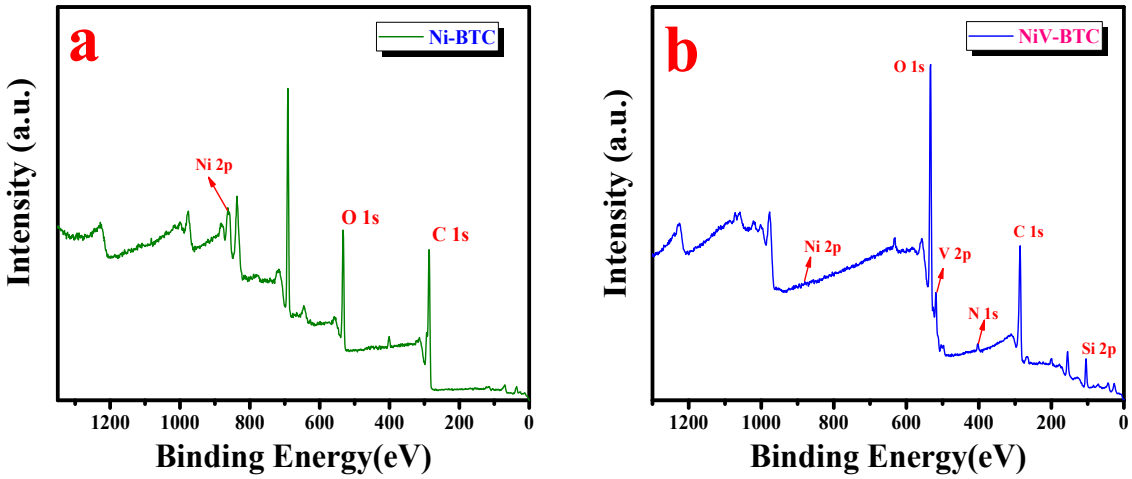

Figure S4: (a-b) XPS survey spectra of Ni-BTC and NiV-BTC respectively.

Table T1: Atomic percentage of Ni-BTC and NiV-BTC via ICP-MS analysis.

Atomic %	C	O	Ni	V
Ni-BTC	**56.71**	**18.18**	**25.1**	**-**
NiV-BTC	**46.34**	**36.99**	**10.26**	**4.46**

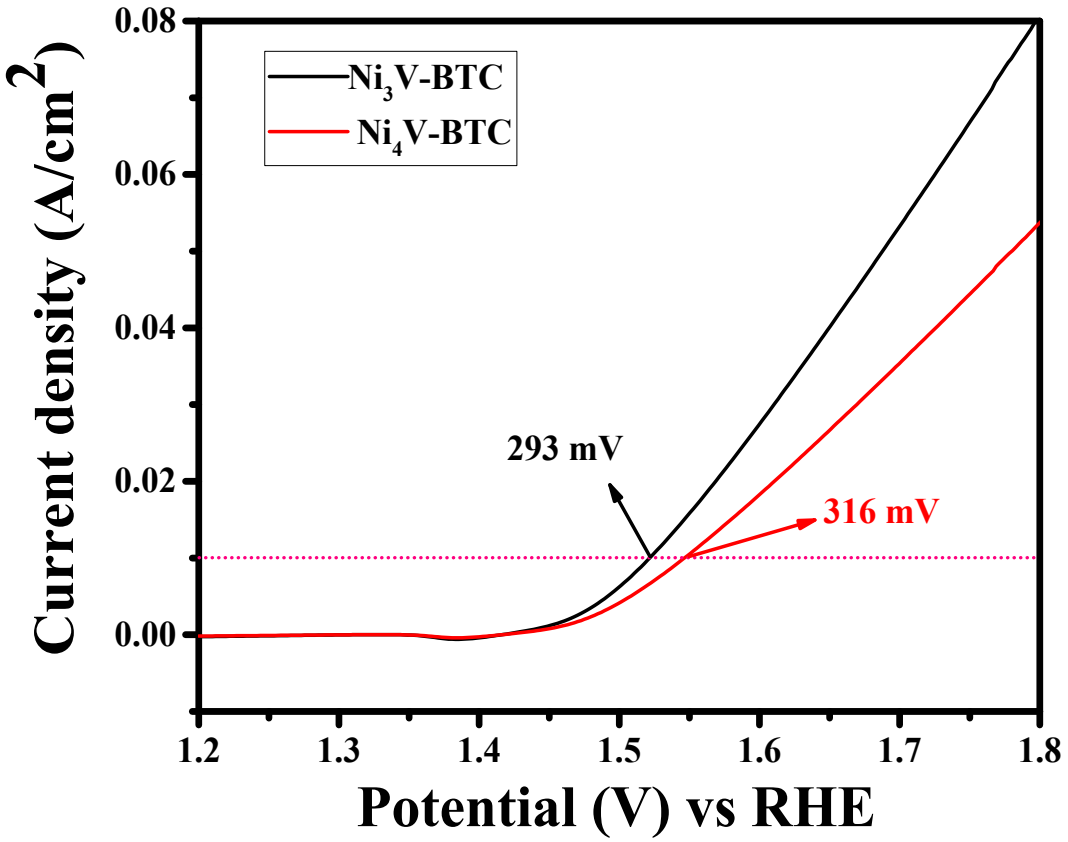

Figure S5: LSV polarization curve obtained at a scan rate value of 5 mV s^{-1} for different catalysts.

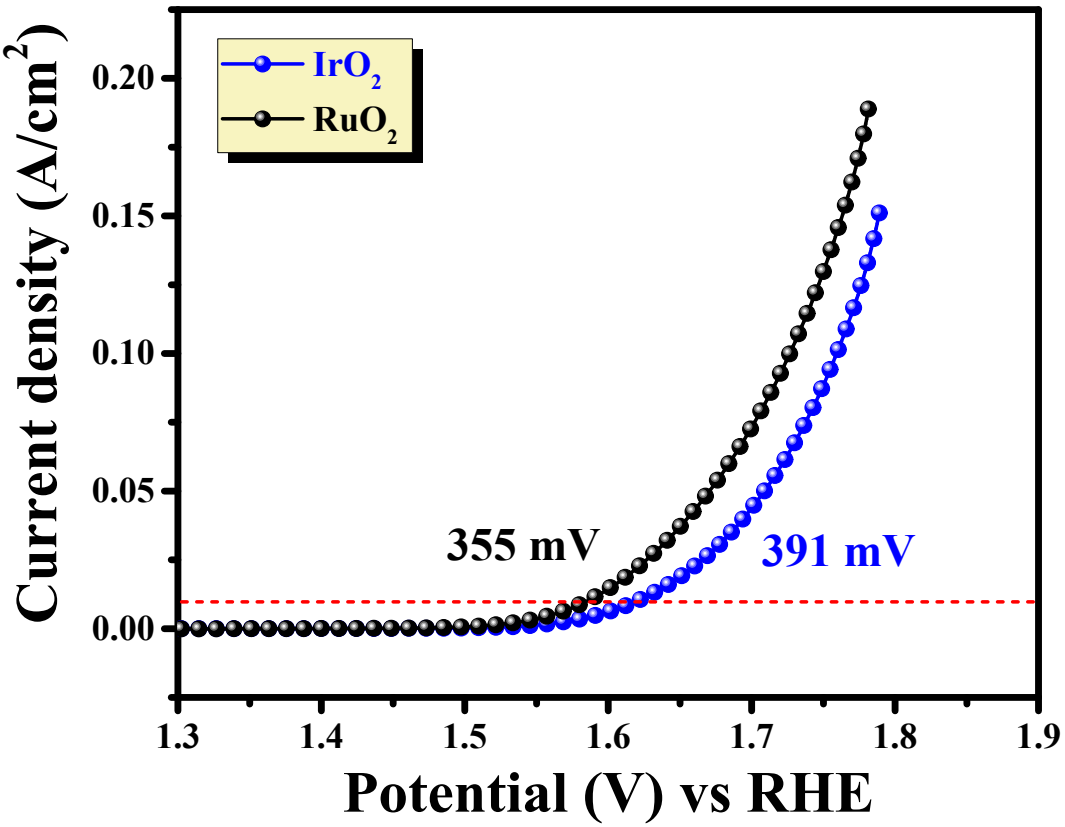

Figure S6: LSV polarization curve for RuO_2 and IrO_2 in 1 M KOH solution.

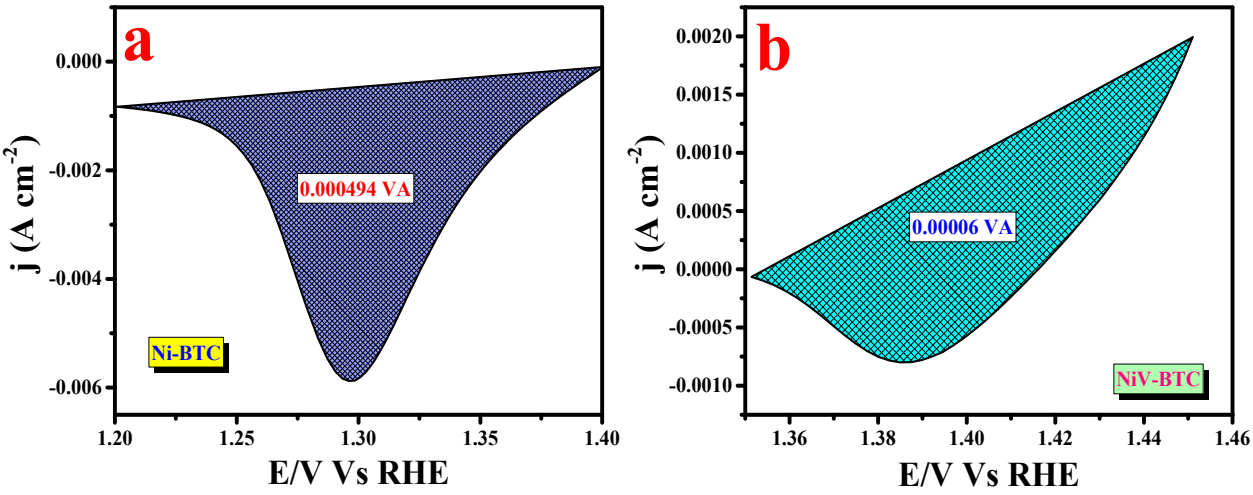

Figure S7: (a) and (b) Reduction area of Ni-BTC and NiV-BTC respectively.

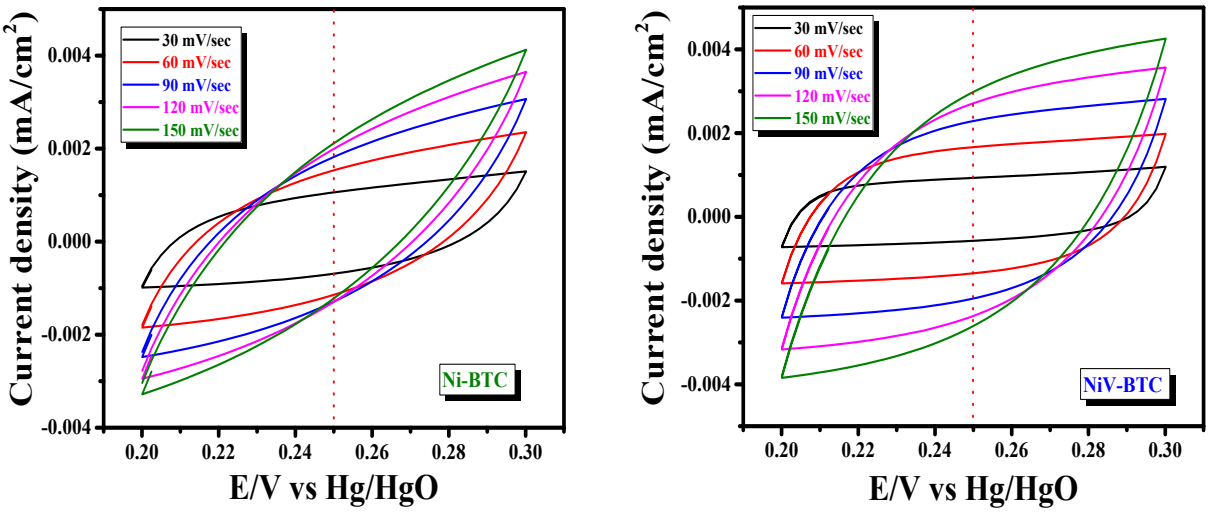

Figure S8: (a) and (b) CVs recorded in a non-faradaic region with increasing scan rate for the determination of ECSA from its double layer capacitance for Ni-BTC and NiV-BTC respectively.

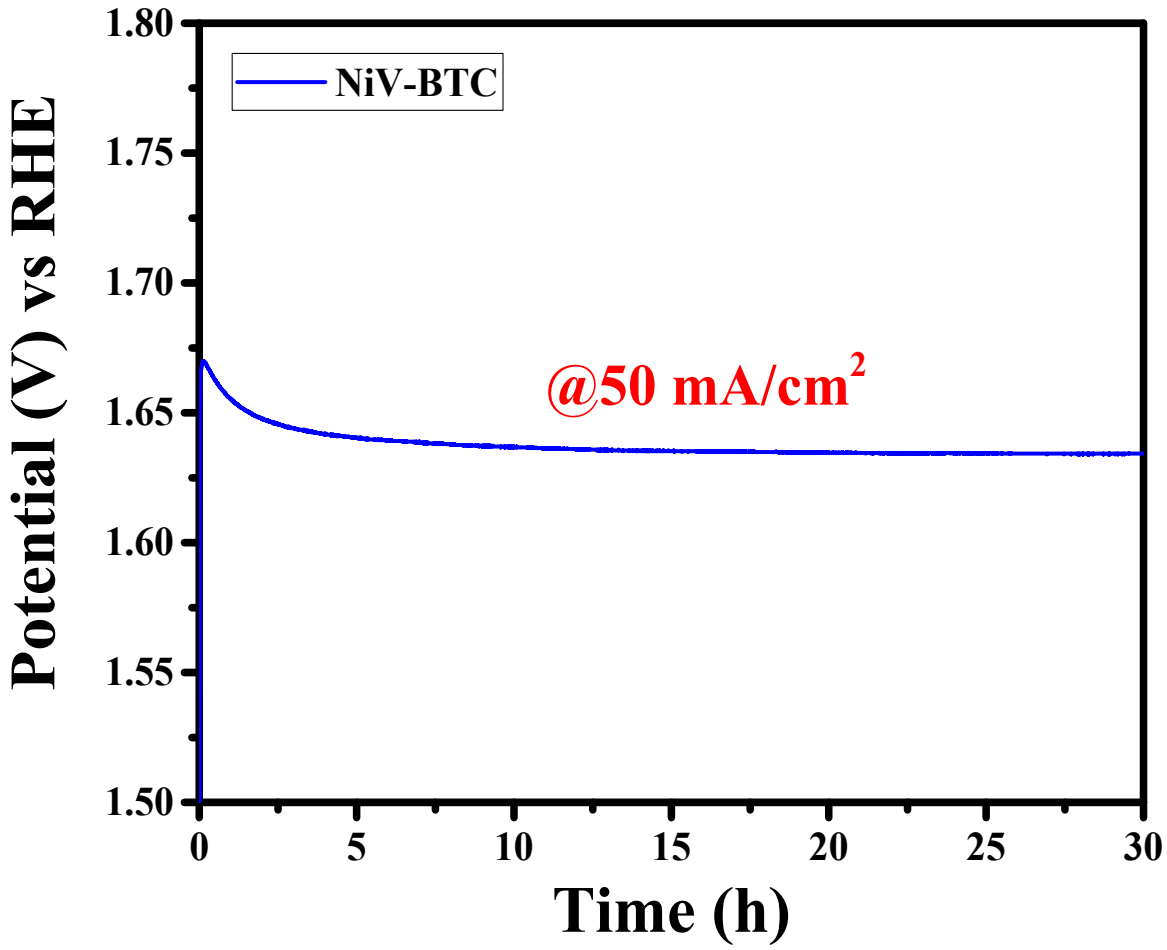

Figure S9: Chronopotentiometric outcomes of NiV-BTC @50 mA/cm^2 for 30 h in 1 M KOH solution.

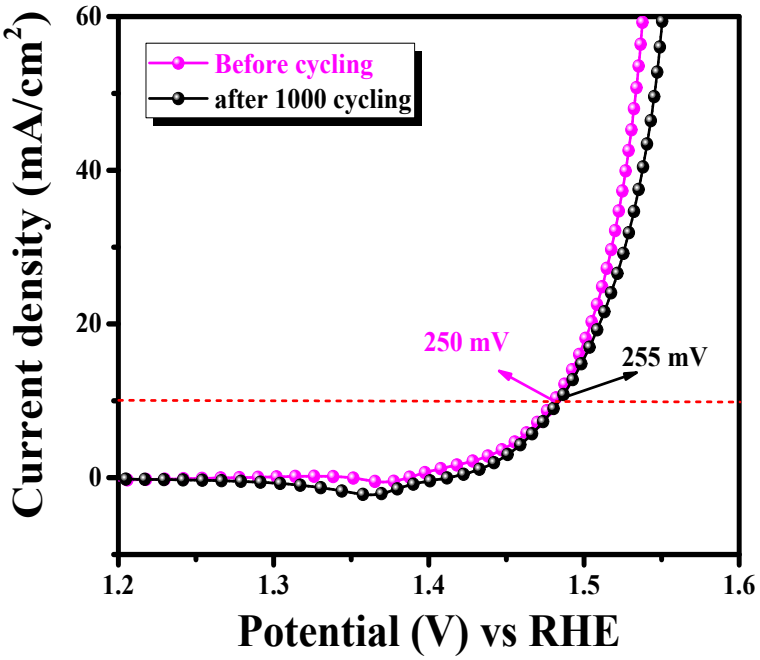

Figure S10: LSV polarization curves for NiV-BTC before and after AD study.

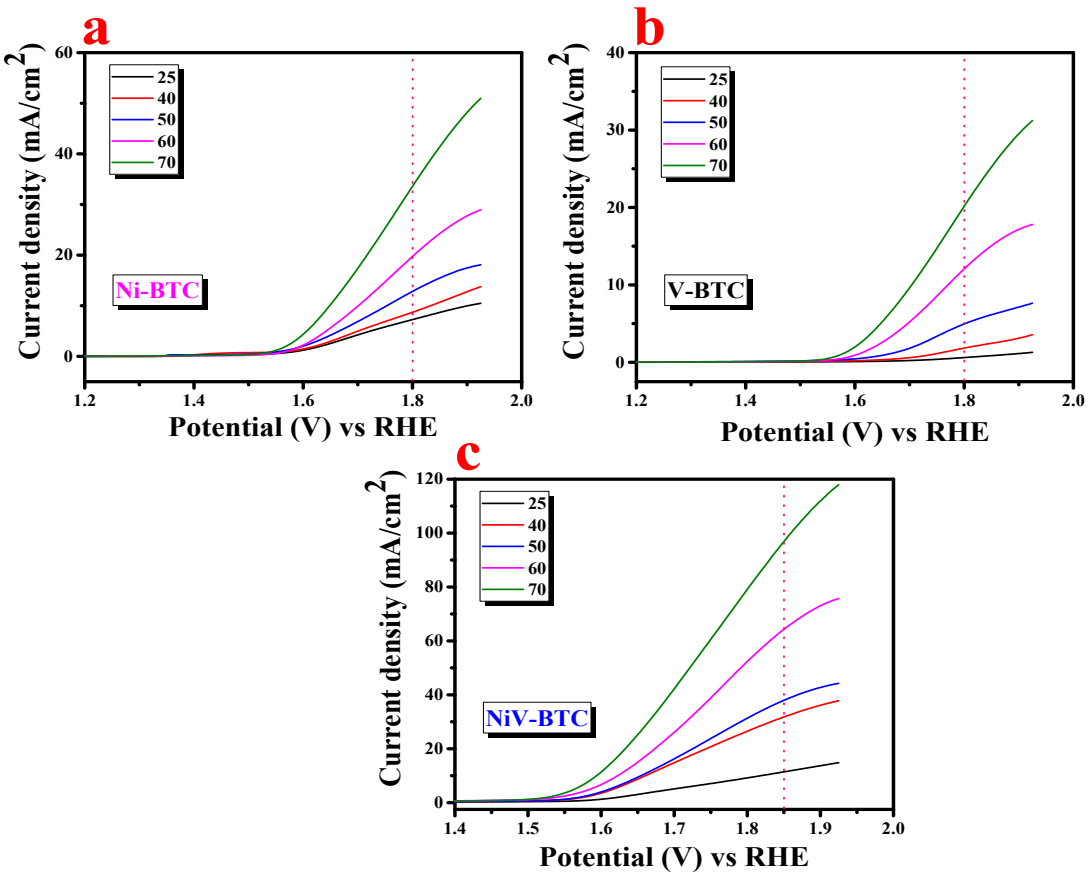

Figure S11: (a), (b) and (c) LSV plots at various temperatures for Ni-BTC, V-BTC and NiV-BTC respectively.

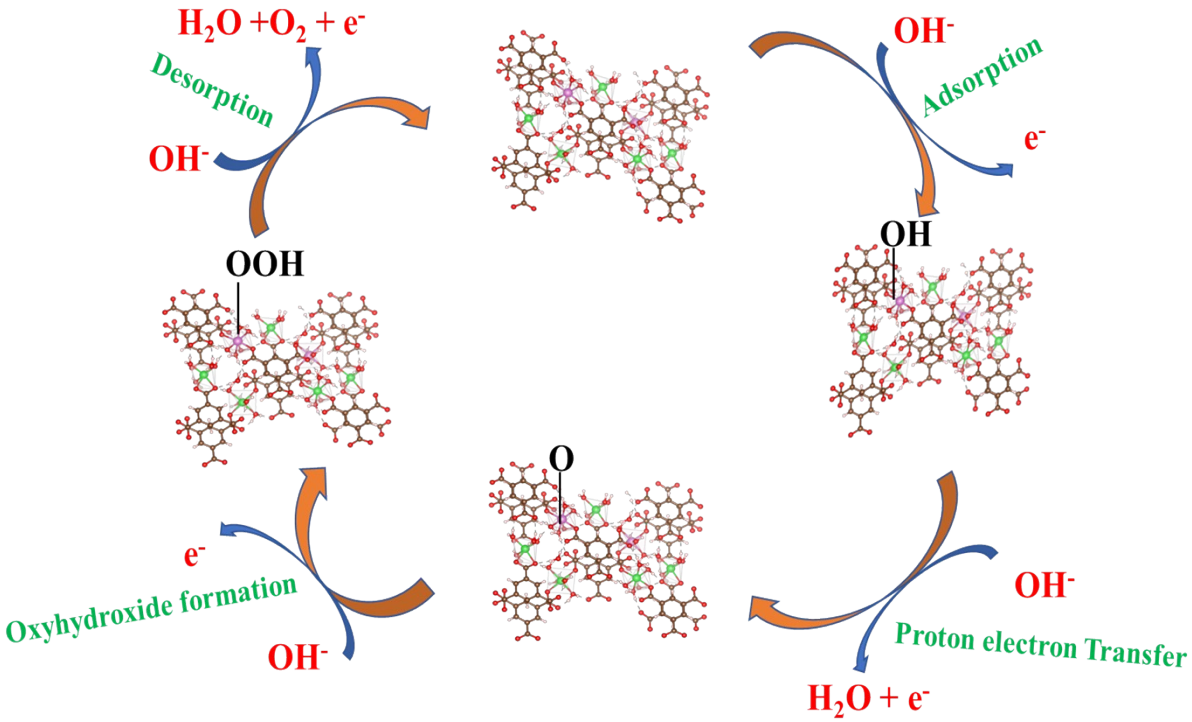

Figure S12: OER process includes adsorption, dissociation and desorption steps.

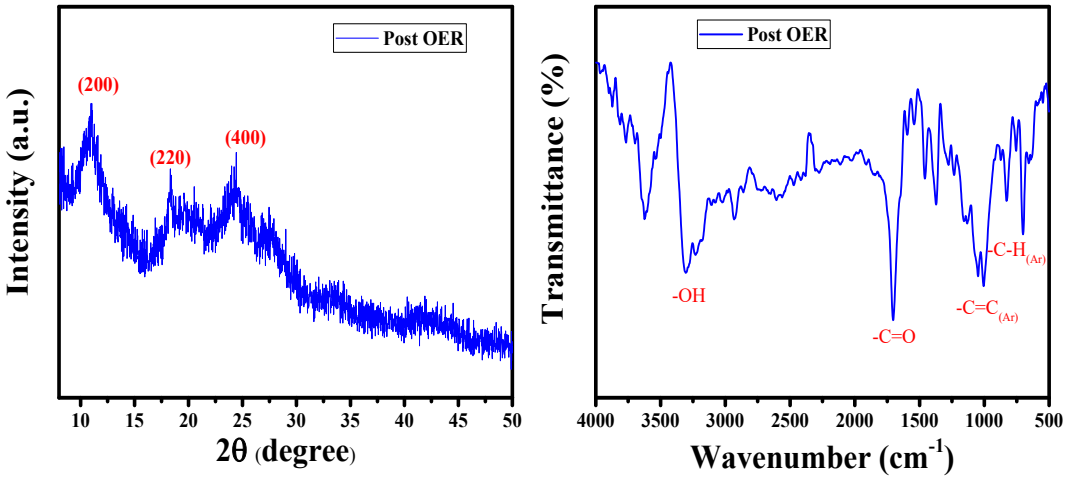

Figure S13: (a) XRD plot and (b) IR study after OER study of NiV-BTC respectively.

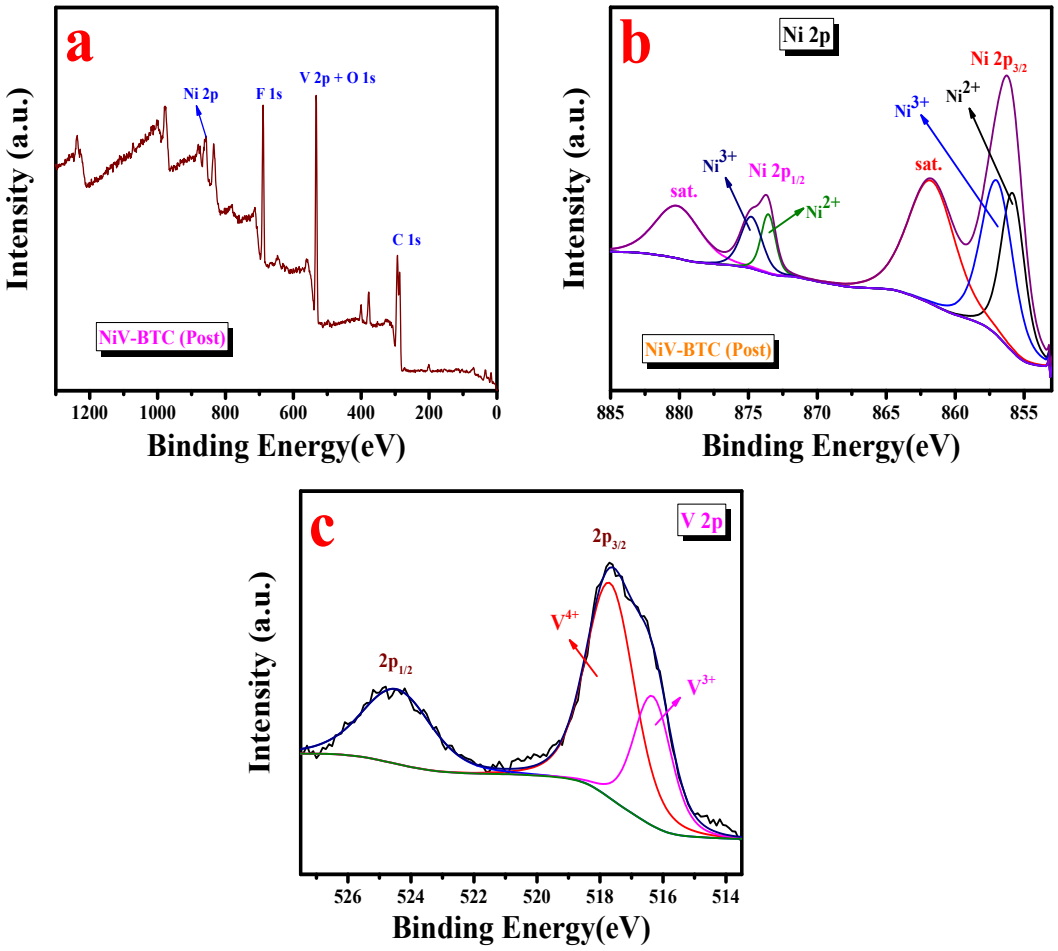

Figure S14: (a), (b) and (c) Post XPS survey spectra, Ni 2p and V 2p orbital of NiV-BTC respectively.

Table T2: Comparison table of OER catalytic performances of previously reported similar MOF-based electrocatalysts.

Sl. No	Catalysts	j (mA cm^{-2})	η (mV)	Tafel Slope (mV/dec)	Stability	Electrolyte	Ref.
1	Ni−Fe−P-350	10	271	53	10 h	1.0 M KOH	1
2	NiFe/N-CNT	10	290	79	-	0.1 M KOH	2
3	Ir@Ni-NDC	10	210	44.7	100 h	1.0 M KOH	3
4	2D MOF-Fe/Co (1:2)	10	238	52	50000 s	1.0 M KOH	4
5	3D Ni_2P@C/ NF	10	205	63	48 h	1.0 M KOH	5
6	Ni-BTC-MWCNT	10	243	57	23 h	1.0 M KOH	6
7	$Ni_{0.1}Co_{0.9}$-MOF	100	384	46.4	20 h	1.0 M KOH	7
8	Ni-BTC/CC	10	441	123.7	-	1.0 M KOH	8
9	NiCo-Bpy-BTC	10	292	38	16 h	1.0 M KOH	9
10	FCN-BTC MOF	10	218	29.3	24 h	1.0 M KOH	10
11	Ni_2V-MOFs@NF	10	244	56	80 h	1.0 M KOH	11
12	**NiV-BTC**	**10**	**250**	**51**	**30 h**	**1.0 M KOH**	**This work**

References

1 C. Xuan, J. Wang, W. Xia, Z. Peng, Z. Wu, W. Lei, K. Xia, H. L. Xin and D. Wang, *ACS Appl Mater Interfaces*, 2017, **9**, 26134–26142.

2 H. Lei, Z. Wang, F. Yang, X. Huang, J. Liu, Y. Liang, J. Xie, M. S. Javed, X. Lu, S. Tan and W. Mai, *Nano Energy*, 2020, **68**, 104293.

3 J. Yang, Y. Shen, Y. Sun, J. Xian, Y. Long and G. Li, *Angewandte Chemie - International Edition*, , DOI:10.1002/anie.202302220.

4 K. Ge, S. Sun, Y. Zhao, K. Yang, S. Wang, Z. Zhang, J. Cao, Y. Yang, Y. Zhang, M. Pan and L. Zhu, *Angewandte Chemie - International Edition*, 2021, **60**, 12097–12102.

5 N. Chen, S. Che, H. Liu, G. Li, N. Ta, F. Jiang Chen, B. Jiang, N. Wu, Z. Li, W. Yu, F. Yang and Y. Li, *J Colloid Interface Sci*, 2023, **638**, 582–594.

6 S. Kiran, K. Jabbour, G. Yasmeen, Z. Shafiq, A. Abbas, S. Manzoor, J. Hussain, A. Al-Harrasi, M. A. Bajaber, A. H. Ragab and M. N. Ashiq, *Appl Organomet Chem*, 2023, 1–14.

7 J. Cai, Z. Xu, X. Tang, H. Liu, X. Zhang, H. Li, J. Wang and S. Li, *J Alloys Compd*, 2023, **947**, 169498.

8 S. Naik Shreyanka, J. Theerthagiri, S. J. Lee, Y. Yu and M. Y. Choi, *Chemical Engineering Journal*, 2022, **446**, 137045.

9 B. Ambrose, R. Madhu, A. Kannan, S. Senthilvel, M. Kathiresan and S. Kundu, *Electrochim Acta*, 2023, **439**, 141714.

10 Z. Li, S. Deng, H. Yu, Z. Yin, S. Qi, L. Yang, J. Lv, Z. Sun and M. Zhang, *J Mater Chem A Mater*, 2022, **10**, 4230–4241.

11 J. Lv, P. Liu, F. Yang, L. Xing, D. Wang, X. Chen, H. Gao, X. Huang, Y. Lu and G. Wang, *ACS Appl Mater Interfaces*, 2020, **12**, 48495–48510.